Supplementary material

Supplementary material 1. Normalization

Firstly, we had explored the signal consistency of the fat in the same phase direction with lesions in all patients with multiple myeloma (MM) (*Figure S1*). Two radiologists (S Xia, X Ji with 22 and 10 years of experience) drew the signal of each lesion, normal bone marrow, and subcutaneous fat at the same level in T1-weighted water-fat separation Dixon.

Secondly, we verified the normal distribution of subcutaneous fat signal, drew the histogram, then tested the consistency between the two radiologists.

Third, the signal intensity on both water and fat phase drawn by two radiologists showed normal distribution (*Figure S2*).

Fourth, the subcutaneous fat signals measured by the two observers were highly consistent, R^2=0.936, 0.926 (*Figure S3*).

Thus, we used the subcutaneous fat signal as a reference to the lesions.

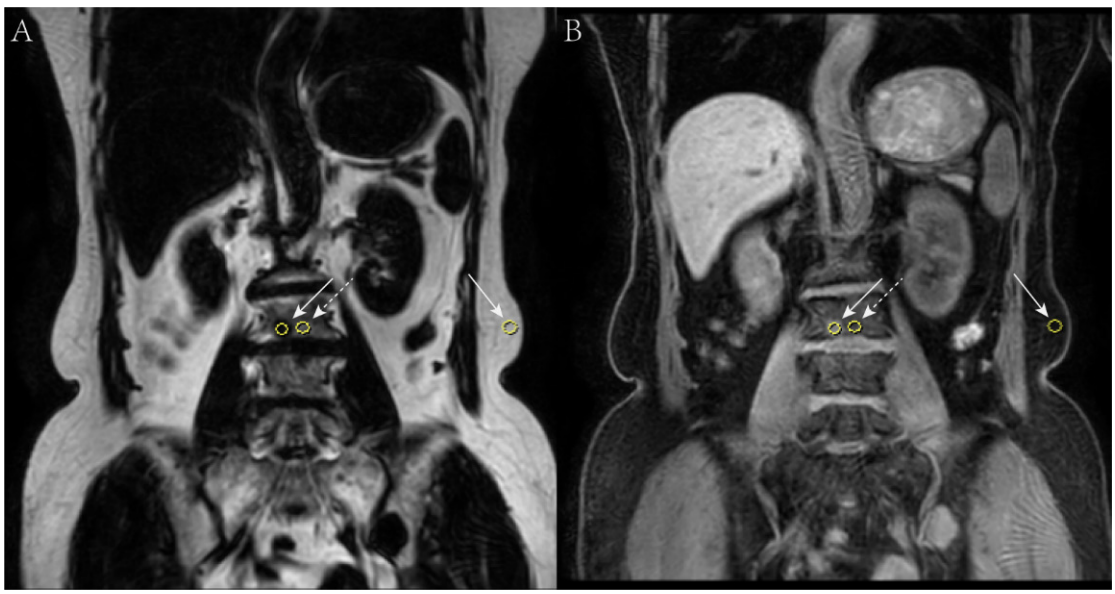

Figure S1 The coronal fat phase image of the thoracolumbar spine shows the focal lesion (the solid arrow), NABM of the same vertebral body (the virtual arrow), subcutaneous fat of the same vertebral body (another solid arrow) (A); the coronal water phase image of the thoracolumbar spine shows the focal lesion (the solid arrow), NABM of the same vertebral body (the virtual arrow), subcutaneous fat of the same vertebral body (another solid arrow) (B). NABM, normal-appearing bone marrow.

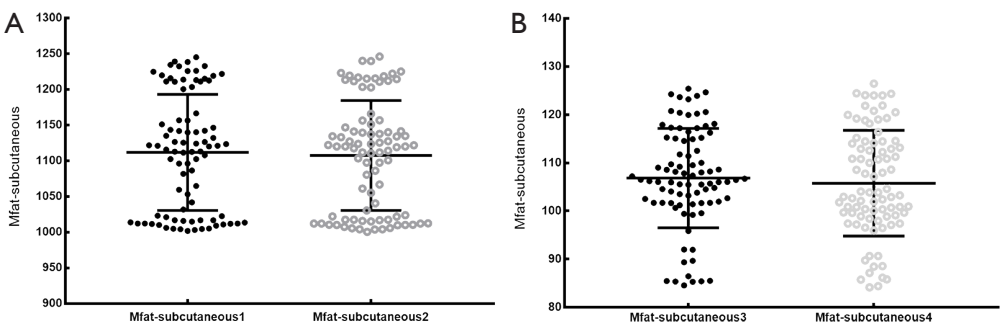

Figure S2 The signal intensity on both water and fat phase drawn by 2 radiologists showed normal distribution. Mfat, fat signal intensity.

http://dx.doi.org/10.21037/qims-20-289

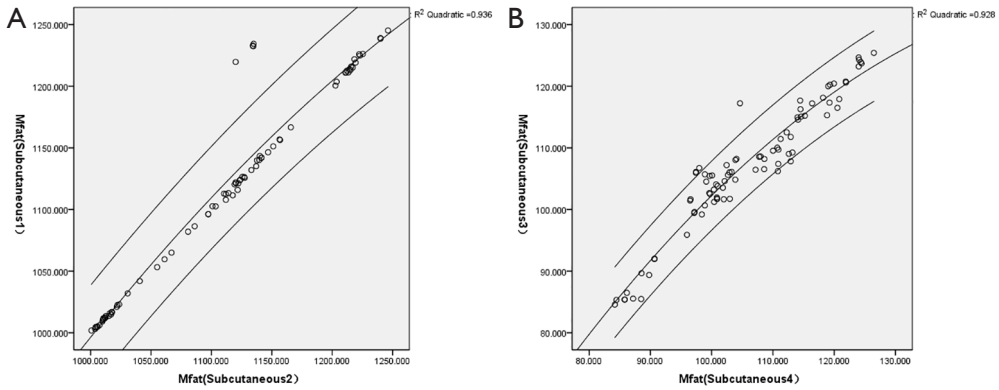

Figure S3 Verification of the inter-group consistency of subcutaneous fat signals sketched by two radiologists. The subcutaneous fat signals measured by the two observers were highly consistent, R^2=0.936, 0.926. Mfat, fat signal intensity.

Supplementary material 2. The selection of FLs on high quality images (Figure S4)

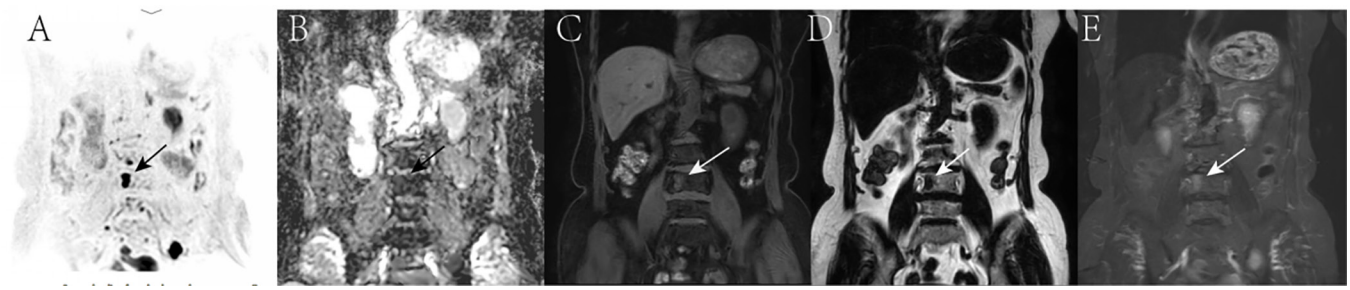

Figure S4 A focal lesion was clearly shown on all sequences. The focal lesion shows hyperintensity on coronal DWI image (A), isointensity on ADC image (B), T2-STIR image (C), hypointensity on fat phase image (D), and water phase image (E). DWI, diffusion-weighted imaging; STIR, short-time inversion recovery; ADC, apparent diffusion coefficient.

Supplementary material 3. The inclusion and exclusion criteria for patients (Figure S5)

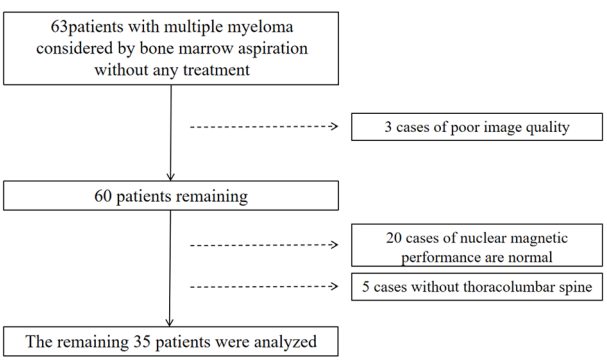

Figure S5 Flowchart of enrolled patients.

http://dx.doi.org/10.21037/qims-20-289

Supplementary material 4. High quality of images

(I) We adopted a standardized scanning scheme and a respiratory gating scheme to ensure a high SNR. (II) We used a high b value (800 s/mm^2) to reduce signal the background tissue. (III) We chose images without motion artifacts and image deformation for analysis. *Figure S6* below shows the high quality of the images (reference: Messiou C, Hillengass J, Delorme S, *et al.* Guidelines for Acquisition, Interpretation, and Reporting of Whole-Body MRI in Myeloma: Myeloma Response Assessment and Diagnosis System (MY-RADS). Radiology 2019;291:5-13).

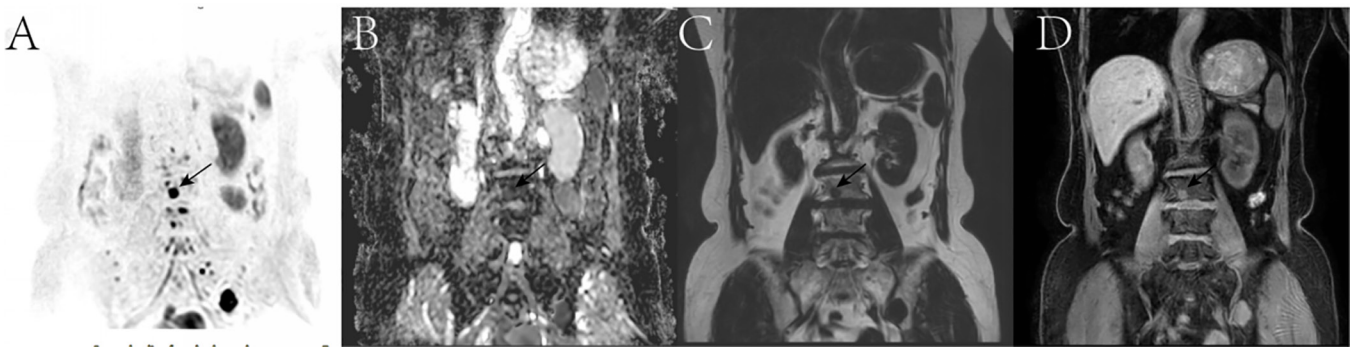

Figure S6 (A,B,C,D) The DWI, ADC, fat phase, and water phase images are displayed respectively. No artifacts were seen and the lesions were clearly shown (arrows). DWI, diffusion-weighted imaging; ADC, apparent diffusion coefficient.

Supplementary material 5. Correlation between MRI parameters of focal lesions and different BMPC (Figure S7)

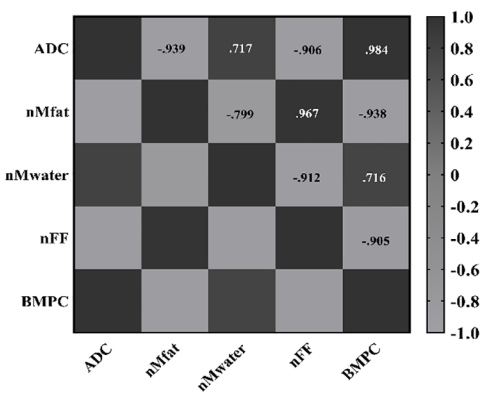

Figure S7 Correlation matrix showed correlation between MRI parameters of FLs and different BMPC. Strong correlation between ADC, nMfat, nMwater, nFF of focal lesions and BMPC was found (P<0.05). BMPC, bone marrow plasma cells; FLs, focal lesions; ADC, apparent diffusion coefficient; nMfat, normalized fat signal intensity; nMwater, normalized water molecular signal intensity; nFF, normalized fat fraction.

http://dx.doi.org/10.21037/qims-20-289

Supplementary material 6 (Table S1)

Table S1 The clinical and biological data of the enrolled patients

Patient	Gender	Age (years)	BMPC (%)	Cr (μmol/L)	HGB (g/L)	Ca (mmol/L)	Treatments received
1	1	60	1.5	44.4	110	2.2	TAD
2	0	50	2	71	129	2.37	RD
3	0	69	4	110.5	138	3.08	BCD
4	0	58	4.06	53	93	2.19	BCD
5	1	66	4.5	87.4	121	2.14	BD
6	1	62	4.9	82.7	100	223	MPR
7	1	61	5.2	73	112	1.82	PAD
8	1	36	5.5	77.5	134	2.52	BCD
9	1	65	5.8	64	98	2.13	BCD
10	0	44	6	52.9	134	2.76	BCD
11	0	38	6.5	49.5	137	1.92	BCD
12	1	57	7.5	52.9	134	2.38	MPR
13	1	63	8	66	94	2.35	BCD
14	1	44	8.5	91	100	2.55	BCD
15	0	44	9	66.6	140	2.33	RCD
16	1	44	14	60.7	102	2.33	RCD
17	1	48	20	82.8	95	2.58	BCD
18	1	52	45	94.6	99	2.52	BCD
19	1	67	48	106	101	2.47	BD
20	0	52	50	102.9	124	2.48	BCD
21	1	52	52	72.8	141	2.32	RCD
22	0	45	53	56.1	95	2.21	BD
23	1	54	62	80.1	98	2.41	VTD
24	0	53	66	80.5	96	2.35	RCD
25	0	39	70	119.1	93	3.45	PAD
26	1	63	75	72.8	94	1.86	BCD
27	0	66	78	194.5	95	2.23	BCD
28	0	32	79	56	113	2.21	BD
29	1	58	79.5	237.1	94	1.76	BCD
30	1	36	80	70.5	112	2.18	BCD
31	0	62	81	323.3	98	2.51	TCD
32	0	55	82.3	40.3	93	1.95	BCD
33	0	41	85.5	46.7	136	2.38	TAD
34	1	47	90	22.2	90	2.39	TAD
35	1	52	95	51.6	90	1.75	TCD

Gender, female-0, male-1; BMPC, bone marrow plasma cells; Cr, creatinine; HGB, hemoglobin; Ca, calcium; BCD, bortezomib, cyclophosphamide, dexamethasone); BD, bortezomib, dexamethasone; MPR, melphalan, prednisone, lenalidomide; PAD, bortezomib, adriamycin, dexamethasone; RCD, lenalidomide, cyclophosphamide, dexamethasone; RD, lenalidomide, dexamethasone; TAD, thalidomide, adriamycin, dexamethasone; TCD, thalidomide, cyclophosphamide, dexamethasone; VTD, bortezomib, thalidomide, dexamethasone.

http://dx.doi.org/10.21037/qims-20-289